LA-UR- 01-2818

Approved for public release; distribution is unlimited.

Title: Misfit Dislocations in Epitaxial Ni/Cu Bilayer and Cu/Ni/Cu Trilayer Thin Films

Author(s): Tadashi Yamamoto, MST-8
Amit Misra, MST-8
Richard G. Hoagland, MST-8
Mike Nastasi, MST-8
Harriet Kung, MST-8
John P. Hirth, MST-DO

Submitted to: Proceeding Paper for MRS Spring Meeting, 2001

Misfit Dislocations in Epitaxial Ni/Cu Bilayer and Cu/Ni/Cu Trilayer Thin Films

Tadashi Yamamoto, Amit Misra, Richard G. Hoagland, Mike Nastasi, Harriet Kung, and John P. Hirth
MST-8, Materials Science and Technology Division
Los Alamos National Laboratory, Los Alamos, NM

ABSTRACT

Misfit dislocations at the interfaces of bilayer (Ni/Cu) and trilayer (Cu/Ni/Cu) thin films are examined by plan-view TEM observation. In the bilayers, the spacing of misfit dislocations is measured as a function of nickel layer thickness. The critical thickness, at which misfit dislocations start to appear with the loss of coherency, was found to be about 2 nm. The spacing of the misfit dislocations decreases with increasing nickel layer thickness and reaches a plateau at the thickness of 30 nm. The minimum spacing is observed to be about 20 nm. **g**·**b** analysis of the cross-grid of misfit dislocations revealed 90° Lomer dislocations of <110>{001} type lying in the (001) interface plane at the relatively large thickness of nickel layer, but 60° glide dislocations of <110>{111} type at the relatively small thickness of nickel layer. In the trilayers, misfit dislocations formed at both interfaces. The spacing of the misfit dislocation is in agreement with that of the bilayers with similar nickel layer thickness. The misfit dislocation arrays at the two interfaces, having the same line directions, are 60° dislocations with edge components with opposite signs but are displaced with respect to each other in the two different interface planes. This suggests that the strain field of the dislocations has a strong influence on the position of the misfit dislocations at the subsequent interface.

INTRODUCTION

It is well known that misfit dislocations form in the interface plane to relieve the elastic strains due to lattice mismatch in heteroepitaxial films [1-7]. In the early stages of the overgrowth, the misfit is entirely accommodated by coherency strains, where two lattice planes are strained in one-to-one registry. As the overgrowth thickness increases, the misfit dislocations start forming at the critical thickness, where the introduction of misfit dislocations lower the total energy of the system arising from elastic strain and dislocations [1,2]. Analyses of critical thickness and strain field have been the major subject of both theoretical and experimental studies, where most detailed analyses have been done for semiconductor bilayer couples [2-7]. Once the dislocations form as the thickness exceeds the critical thickness, the dislocation spacing, or strain complementary to the spacing, decreases with either increasing thickness or increasing lattice mismatch [4,5]. For characters of the misfit dislocations, <110>{111} type 60° dislocations are generally observed at relatively small thickness or small lattice mismatch. As the thickness or lattice mismatch increases, a fraction of 60° dislocation decreases and 90° dislocations of <110>{001} type predominantly form [4,5]. It is generally suggested that the 90° dislocation forms by reaction of two 60° dislocations at the interfaces [6,8]. For the metal bilayer systems, fcc metals have been preferably studied in the limited thickness range of 1 to 10 nm [9-15]. Coherency strain and misfit dislocation density in the metal bilayers behave with layer thickness in a similar manner to those in the semiconductor bilayers [10,11]. For the characters

of misfit dislocations, 60° dislocations have been generally observed [9,10], but 90° dislocations have been also reported [11], and no consensus has yet reached. There is a lack of understanding of misfit dislocations in metal bilayers. It is thought that the deformation of the multilayer films is determined by the mutual interaction between gliding dislocations and misfit dislocations in the interfaces. For example, the misfit dislocations locked in the interfaces behave to block the motion of gliding dislocations [12]. Spacing between two pinned dislocations at the interfaces determines the strength by Orowan type relation. Thus far, systematic measurement of spacing vs. layer thickness has not been found in any literature. In this view, comprehensive understanding of the nature of misfit dislocations as a function of layer thickness is of prime interest in the fabrication of high-strength multilayers. In this research, we investigate the critical thickness, spacing, configurations, Burgers vectors, and characters of misfit dislocations between two layers by changing the thickness of the overgrowth nickel layer in the Ni/Cu bilayers and Cu/Ni/Cu trilayer.

EXPERIMENT

Copper and nickel layers are prepared by sequential evaporation of high-pure metals (99.999%) using electron beam evaporator (ESV 6/UHV, Leybold-Heraeus) and grown cube-on-cube onto the (001) surface of NaCl, cleaved in air. Then the chamber was evacuated to the high vacuum ($7x10^{-8}$ Torr). Then, the substrate was heated up to 350 °C and was held at this temperature for about two hours, which helps to remove the air trapped on the NaCl surface [13]. 100 nm thick layer of copper was first grown along [001] on the NaCl substrate at 350 °C. After the substrate was cooled down to 50 °C, a nickel layer was deposited onto the surface of copper, parallel to (001) plane, at the desired thickness from 2 to 70 nm. During the evaporation, the pressure in the chamber dropped between $3x10^{-7}$ and $3x10^{-6}$ Torr, but after the deposition, the pressure quickly recovered to the level of the base pressure. The bilayer crystals were removed from the vacuum chamber after they had cooled down to the room temperature. Both copper and nickel layers were grown at relatively low growth rate of 0.08 nm/s to minimize the residual stress induced possibly by the bombardment of energetic vapor atoms [14]. Thickness and evaporation rate were monitored by a quartz crystal oscillator (XTC, Inficon). The thickness was also checked by the cross-sectional TEM observation. The 70 nm Cu/10 nm Ni/70 nm Cu trilayer was fabricated in the similar manner except that the additional third copper layer was grown at 50 °C right after the deposition of the nickel layer. The films were floated off the NaCl in the distilled water at room temperature. The films were carefully mounted onto the 3 mm double-folded Cu grid for the TEM analysis of the misfit dislocations. Both bright field and dark field images were taken by Philips CM30 operated at 300 kV. Liquid nitrogen cooled anti-contaminator was used throughout the observation.

DISCUSSIONS

Bilayers

Electron micrographs of 10 nm Ni/100 nm Cu and 70 nm Ni/ 100 nm Cu bilayers, taken with 200 type reflections, are shown in Figure 1. The foils are oriented approximately along the

[001] direction. The misfit dislocation lines are straight and parallel to [220] and [2$\underline{2}$0] directions and form the cross-grid arrays. The misfit dislocation spacing in the 10 nm thick nickel varies between 30 and 60 nm (Figure 1(A)) and the spacing in 70 nm thick nickel is between 10 and 25 nm (Figure 1(B)). The average spacings of 10 nm nickel and 70 nm nickel are about 40 and 20 nm respectively. It is also noted that the variation of the spacing is larger in the 10 nm nickel layer than in 70 nm layer. Measuring the misfit dislocation spacing from several areas for each sample, the spacing was plotted as a function of nickel layer thickness (Figure 2). We still observed misfit dislocations at 5 nm thick nickel layer, but no misfit dislocations were observed at 2 nm nickel layer. Thus, the critical thickness is thought to be between 2 and 5 nm. As the nickel layer thickness increases, the spacing of misfit dislocations decrease quickly until the thickness reaches 30 nm. As the thickness further increases, the spacing gradually decreases and approaches asymptotically to the equilibrium value of 20 nm. **g·b** analysis has been performed to reveal the Burgers vectors and characters of the misfit dislocations. Most of the dislocations observed in the 10 nm Ni/100 nm Cu bilayer sample are 60° glide dislocations of <110>{111} type. However, in the 30, 50, 70 nm Ni/ 100 nm bilayer we observed that most dislocations are Lomer-Cottrell dislocations of <110>{001} type lying on the (001) interface plane.

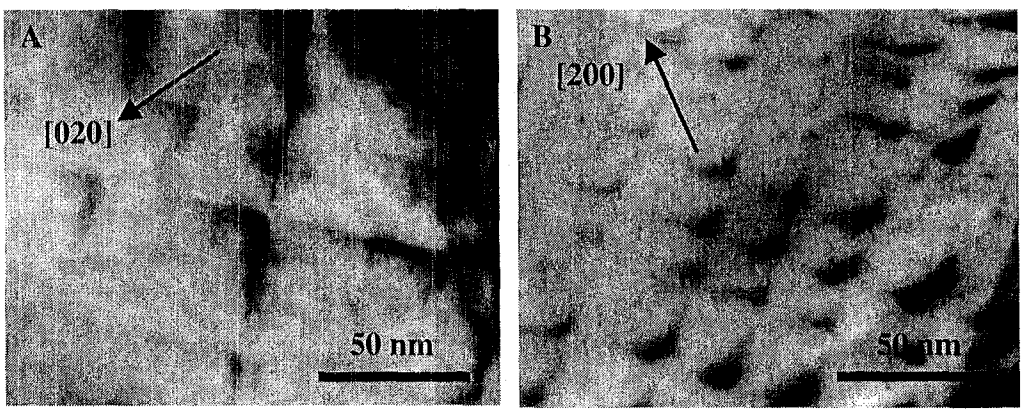

Figure 1. Misfit dislocations at (A) 10 nm Ni and (B) 70 nm Ni epitaxially deposited on 100 nm copper layer.

Matthews and Crawford [10] studied misfit dislocations in Ni/Cu bilayers prepared by evaporation and measured the elastic strains varying the nickel thickness h from 1 to 9 nm. They observed that the dislocation density increased with increasing thickness of the nickel overgrowth layer, although no measurement of spacing or density of misfit dislocations was conducted. They also found <110>{111}-type 60° dislocations lying on the glide plane which is consistent with our results for h = 10 nm. 60° dislocations have been consistently observed for other fcc metal bilayers such as β-Co/Cu [9], and Pt/Au [15]. Their critical thickness h_c was about 1.46 nm and their theoretical calculation gives h_c = 1.9 nm, compared well to our result. The trend of the dislocation spacing vs. layer thickness in the current study is consistent with their observation. Burgers vectors of the misfit dislocations are also in agreement at least over the thickness range (< 10 nm). Transition of characters of the misfit dislocations with increasing h can be understood by knowing the fact that 90° dislocations accommodate the lattice misfit more efficiently than 60° dislocations. However, the formation mechanisms of the two different

types of misfit dislocations with variation of layer thickness will need to be elucidated from the point of nucleation and stability of the dislocations.

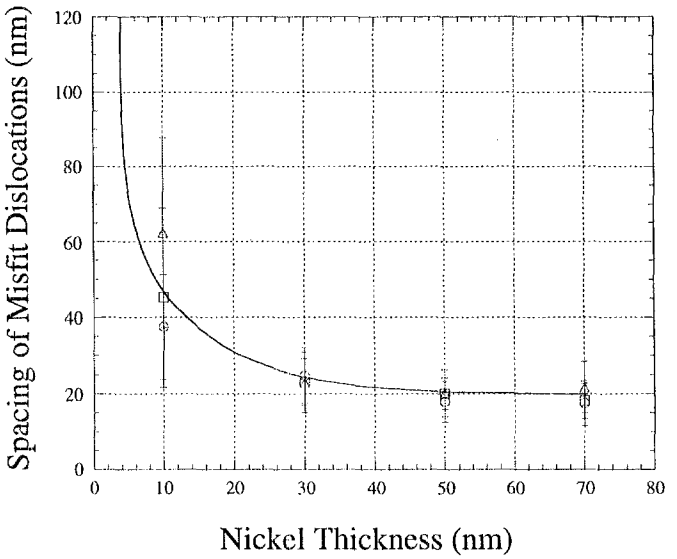

Figure 2. Spacing of misfit dislocations with changing thickness of nickel layer epitaxially deposited on 100 nm copper layer.

Coherency strains and stresses can be calculated from the measured spacing of misfit dislocations under the suitable assumptions. For the uniformly strained bilayer, biaxial plane-stress may be applied, $\sigma_{11} = \sigma_{22} = \sigma$, $\sigma_{33} = 0$, and $\varepsilon_{11} = \varepsilon_{22} = \varepsilon$ [8,16,17]. In the isotropic elasticity, $\sigma = 2\varepsilon\mu(1+\nu)/(1-\nu)$, where μ is a shear modulus and ν is a Poisson's ratio. For the bilayer A/B with lattice constants $a_B > a_A$, $|\varepsilon_A| + |\varepsilon_B| + \varepsilon_b = f$, $f = 2(a_B - a_A)/(a_B + a_A)$, $\varepsilon_b = b/\lambda$, total strain $= |\varepsilon_A| + |\varepsilon_B|$, where f is a lattice misfit, b is an edge component on the interface plane of the Burgers vector, and λ is the spacing of the misfit dislocations. Further assuming $|\varepsilon_A| = |\varepsilon_B| = \varepsilon$, $\mu_A = \mu_B = \mu$ and $\nu_A = \nu_B = \nu$ for A and B layers, strain and stress near the interface are obtained by $\varepsilon = (f - \varepsilon_b)/2$ and $\sigma = 2\varepsilon\mu(1+\nu)/(1-\nu)$. Using average values of Ni and Cu for μ, ν, b, and f ($\mu = 74.7$ GPa, $\nu = 0.30$, $b = 0.2524$ nm, $f = 0.0256$; $a_{Ni} = 0.35238$ nm, $a_{Cu} = 0.36150$ nm, $\mu_{Ni} = 94.7$ GPa, $\mu_{Cu} = 54.6$ GPa, $\nu_{Ni} = 0.276$, $\nu_{Cu} = 0.324$), stresses and strains vs. nickel layer thickness can be calculated (Table 1). In this approximation, total strain is divided by the same amount between nickel and copper layers. Therefore, the total strain is twice of the strain in each layer. At 2 nm, near the critical thickness, the misfit is entirely accommodated by the coherency strains of two layers and the stress is as high as 3.55 MPa at 2.56 % strain. At 10 nm formation of misfit dislocations is energetically favored and replace part of the coherency strain, where the coherency stress is 3.11 MPa at 2.24 % strain. At the relatively small thickness, 60° dislocations, which have half of edge component of 90° dislocations along the interface, form to remove the misfit. As the thickness increases, 90° dislocations appear to remove the misfit more efficiently and finally the balanced state is reached between dislocation density and coherency strain. At this thickness, misfit dislocations accommodate about half of the misfit and still the lattice remains strained by 1.22 %, corresponding to the stress of 1.69 MPa, which is higher than values (~0.7 %) reported by Matthews and Crawford [10]. Their strains were obtained by measuring the moiré fringes caused by misfit averaged over the thickness of bilayer. Therefore, it may not

represent the actual strain at the interface, which is considered to be the largest. There are uncertainties about the lattice misfit values used for this calculation. The lattice constants and elastic constants used for the calculation are values in literature, but thin films may have different properties from the bulk properties at the interfaces. Measurement of both strains and spacing is necessary to fully understand the underlying physics. In future, actual strain measurement by X-ray diffraction is awaited.

Table 1. Coherency stress and strain calculated from the spacing of misfit dislocations.

Ni thickness (nm)	Strain	Stress (GPa)
2	0.026	3.6
10	0.022	3.1
30	0.015	2.1
50	0.013	1.8
70	0.012	1.7

Trilayer

In the trilayer Cu/Ni/Cu, we expect that misfit dislocations form at both interfaces and it is interesting to see how the misfit dislocations are arranged at the interfaces as a result of interaction between them. Figure 3(A) shows the typical example of the misfit dislocations in the trilayer 70 nm Cu/10 nmNi/70 nm Cu. Misfit dislocations form a cross-grid of arrays as for the case of the 10 nm Ni/100 nm Cu bilyer.

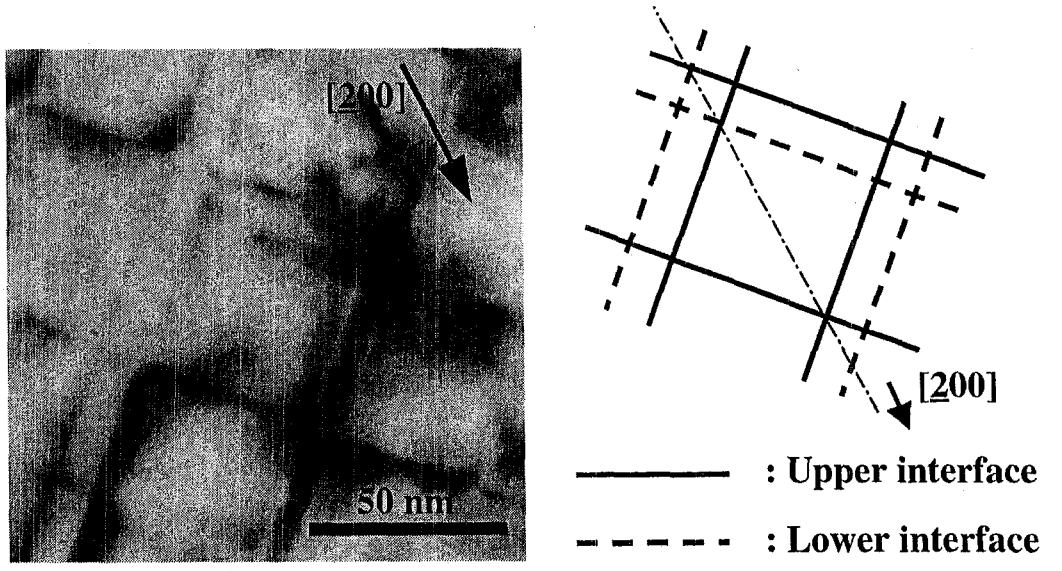

Figure 3. Misfit dislocations in the 20 nm Cu/10 nm Ni/70 nm Cu trilayer. Tilting experiment revealed the arrangement of the paired misfit dislocations.

More interestingly, parallel dislocations are often observed in pairs. The paired dislocations are 60° dislocations whose edge components in the interface have opposite signs. In order to identify the configuration of the paired dislocations, tilting experiment was performed to observe the change of the width of the pair of the dislocations. For the paired dislocation lines crossing in mutually perpendicular directions, their width changes are best observable by tilting along the [200] in the (001) plane. The configuration of the misfit dislocations has been successfully determined. The dislocations designated by the solid lines are located on the upper interfaces, those designated by the dotted lines on the lower interface (Figure 3(B)). Here only one case for trilayers was presented, but study of misfit dislocations in the trilayer with different nickel layer thickness will be planned in future.

CONCLUSIONS

In the bilayers, spacing of misfit dislocations depends on the thickness of nickel layer. Critical thickness is found between 2 and 5 nm. Equilibrium spacing is about 20 nm, larger than the value (~10 nm) corresponding to the lattice misfit. Misfit dislocations accommodated about half of the total misfit. At large nickel overlayer thickness (~30 nm), misfit dislocations are <110>{001} type edge dislocations. At relatively smaller nickel layer thickness (~10 nm), <110>{111} type–60° mixed dislocations are observed lying along the intersection of the {111} slip plane and the {001} interface plane, in both Ni/Cu bilayer and Cu/Ni/Cu trilayer films.

In the trilayer, the misfit dislocation arrays at the two interfaces, having the same line directions, are 60° dislocations with opposite edge components. Paired dislocations were formed on the two interface planes and displaced with respect to each other.

REFERENCES

1. F.C. Frank and J.H. van der Merwe, Proc. Roy. Soc. (London), A198, 216 (1949).
2. J.W. Matthews and A.E. Blakeslee, J. Cryst. Growth, 27, 118 (1974).
3. R. People and J.C. Bean, Appl. Phys. Lett., 47, 323 (1985).
4. R. Hull and J.C. Bean, J. Vac. Sci. Technol., A7, 2580 (1989).
5. J. Petruzzello, B.L. Greenberg, D.A. Cammack, and R. Dalby, J. Appl. Phys., 63, 2299 (1988).
6. J.S. Ahearn and C. Laird, J. Mater. Sci., 12, 699 (1977).
7. H.-J. Gossman, B.A. Davidson, G.J. Gualtieri, G.P. Schwatz, A.T. Macrander, S.E. Slusky, M.H. Grabow, and W.A. Sunder, J. Appl. Phys., 66, 1687 (1989).
8. J. Narayan, S. Sharan, A.R. Srivasta, and A.S. Nandedkar, B1, 105 (1988).
9. J.W. Matthews, Thin Solid Films, 5, 369 (1970).
10. J.W. Matthews and J.L. Crawford, Thin Solid Films, 5, 187 (1970).
11. K. Shinohara and J.P. Hirth, Thin Solid Films, 16, 345 (1973).
12. J.D. Embury and J.P. Hirth, Acta. Metall. Mater., 42, 2051 (1994).
13. J.W. Matthews, J. Vac. Sci. Tech., 3, 133 (1966).
14. Unpublished work.
15. J.W. Matthews and W.A. Jesser, Acta. Metall., 15, 595 (1967).
16. J.P. Hirth and X. Feng, J. Appl. Phys., 67, 3343 (1990).
17. X. Feng and J.P. Hirth, J. Appl. Phys., 72, 1386 (1992).